# Marine heatwaves off eastern Tasmania: Trends, interannual variability, and predictability

**Article** *in* Progress In Oceanography · February 2018

DOI: 10.1016/j.pocean.2018.02.007

CITATIONS
15

READS
522

**6 authors**, including:

Eric C. J. Oliver
Dalhousie University
**58** PUBLICATIONS **1,138** CITATIONS
SEE PROFILE

Alistair J. Hobday
The Commonwealth Scientific and Industrial Research Organisation
**370** PUBLICATIONS **12,838** CITATIONS
SEE PROFILE

Neil J. Holbrook
University of Tasmania
**118** PUBLICATIONS **4,121** CITATIONS
SEE PROFILE

Scott D. Ling
University of Tasmania
**73** PUBLICATIONS **3,396** CITATIONS
SEE PROFILE

Progress in Oceanography 161 (2018) 116–130

Contents lists available at ScienceDirect

Progress in Oceanography

journal homepage: www.elsevier.com/locate/pocean

# Marine heatwaves off eastern Tasmania: Trends, interannual variability, and predictability

Eric C.J. Oliver[a,b,c,*], Véronique Lago[a,b,d], Alistair J. Hobday[d], Neil J. Holbrook[a,e], Scott D. Ling[a], Craig N. Mundy[a]

[a] Institute for Marine and Antarctic Studies, University of Tasmania, Hobart, Tasmania, Australia
[b] Australian Research Council Centre of Excellence for Climate System Science, University of Tasmania, Hobart, Tasmania, Australia
[c] Department of Oceanography, Dalhousie University, Halifax, Nova Scotia, Canada
[d] CSIRO Oceans and Atmosphere, Hobart, Tasmania, Australia
[e] Australian Research Council Centre of Excellence for Climate Extremes, University of Tasmania, Hobart, Tasmania, Australia

ARTICLE INFO

*Keywords:*
Extreme events
Climate change
Climate variability
Ocean modelling
Self-organising maps

ABSTRACT

Surface waters off eastern Tasmania are a global warming hotspot. Here, mean temperatures have been rising over several decades at nearly four times the global average rate, with concomitant changes in extreme temperatures – marine heatwaves. These changes have recently caused the marine biodiversity, fisheries and aquaculture industries off Tasmania's east coast to come under stress. In this study we quantify the long-term trends, variability and predictability of marine heatwaves off eastern Tasmania. We use a high-resolution ocean model for Tasmania's eastern continental shelf. The ocean state over the 1993–2015 period is hindcast, providing daily estimates of the three-dimensional temperature and circulation fields. Marine heatwaves are identified at the surface and subsurface from ocean temperature time series using a consistent definition. Trends in marine heatwave frequency are positive nearly everywhere and annual marine heatwave days and penetration depths indicate significant positive changes, particularly off southeastern Tasmania. A decomposition into modes of variability indicates that the East Australian Current is the dominant driver of marine heatwaves across the domain. Self-organising maps are used to identify 12 marine heatwave types, each with its own regionality, seasonality, and associated large-scale oceanic and atmospheric circulation patterns. The implications of this work for marine ecosystems and their management were revealed through review of past impacts and stakeholder discussions regarding use of these data.

## 1. Introduction

Heatwaves are major climate extremes, in both the atmosphere and the ocean, often with devastating impacts on biota and ecosystems. In the ocean, marine heatwaves have led to observable redistributions of marine species, reconfigurations of ecosystems, and economic losses in fisheries and aquaculture industries (Perry et al., 2005; Garrabou et al., 2009; Wernberg et al., 2013; Mills et al., 2013; Oliver et al., 2017a). The surface ocean off eastern Tasmania is a global warming hotspot (Hobday and Pecl, 2014) and local ecosystems face major challenges due to changes in regional oceanography under climate change (Oliver et al., 2014, 2015; Oliver and Holbrook, 2014; Sloyan and O'Kane, 2015). It is likely that global warming has altered the frequency, duration and intensity of marine heatwaves, and will continue to do so in the future. The rate of change in the physical environment could outstrip the capacity of populations, with the exception of very-short lived species, to adapt to the new temperature regime (Visser, 2008; Hoffman and Sgro, 2011; Kelly et al., 2011). Therefore it is important, ecologically and economically, that we understand the historical context and predictability of marine heatwaves.

Marine heatwaves are extreme events in which ocean temperatures are above the normal range for an extended period of time and can cause widespread and significant damage to marine ecosystems (Johnson and Holbrook, 2014; Hobday et al., 2016a). In particular, marine ecosystems accustomed to low temperatures and which are undergoing change due to long-term increases in water temperature, including those around Tasmania, are particularly vulnerable to additional short term environmental shocks such as marine heatwaves. Increasing temperatures, including transient marine heatwaves, may push ecosystems over a "tipping point" (Lenton et al., 2008; Serrao-Neumann

* Corresponding author at: Department of Oceanography, Dalhousie University, Life Sciences Centre Room 5617, 1355 Oxford Street, Halifax, Nova Scotia, Canada. Tel: +1 902 494 2505.
*E-mail address:* eric.oliver@dal.ca (E.C.J. Oliver).

https://doi.org/10.1016/j.pocean.2018.02.007
Received 26 October 2017; Received in revised form 2 February 2018; Accepted 6 February 2018
Available online 07 February 2018
0079-6611/ 

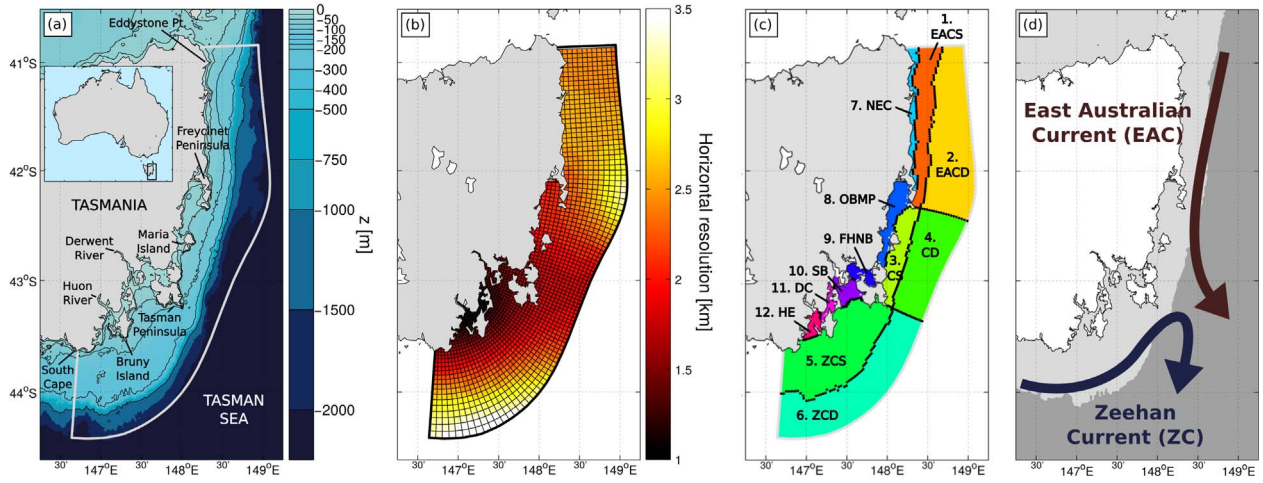


**Fig. 1.** ETAS ocean model (a) domain and bathymetry, (b) curvilinear grid and horizontal resolution, and (c) sub-domain regional definitions. (d) A schematic of the summer (Dec-Jan-Feb) mean surface circulation with the Zeehan Current (ZC) and East Australian Current (EAC) indicated (adapted from Fig. 15 in Oliver et al. (2016)). Region names are East Australian Current-Deep (EACD), East Australian Current-Shelf (EACS), Zeehan Current-Deep (ZD), Zeehan Current-Shelf (ZS), Confluence-Deep (CD), Confluence-Shelf (CS), Northeast Coast (NEC), Oyster Bay & Mercury Passage (OBMP), Frederick Henry and Norfolk Bays (FHNB), Storm Bay (SB), D'Entrecasteaux Channel (DC) and Huon Estuary (HE).

et al., 2016) whereby they enter into a new state which is entirely different from its previous state. This type of tipping point change has been observed in Tasmania whereby marine ecosystems in some regions have changed from habitat-forming highly biodiverse kelp forests to a predominance of low biodiversity sea urchin barrens (Ling, 2008; Johnson et al., 2011). In addition, short-term winter warm spell events, i.e. heatwaves during wintertime, will enable high survival of urchin larvae in the region (Ling et al., 2009b).

Marine heatwaves have occurred off Tasmania's east coast in the past decades and have included impacts on marine ecosystems. A major marine heatwave was observed off southeastern Australia, including coastal Tasmania, in the summer of 2015/16 (Oliver et al., 2017a). This event lasted for 251 days and reached a peak intensity of 2.9 °C above climatology. Apparent impacts included the first outbreak of Pacific Oyster Mortality Syndrome, regional above-average abalone mortality, die-back of bull kelp *Durvillea potatorum* and localised bleaching of crayweed *Phyllospora comosa* (S. Ling, pers. obs.), and out-of-range fish observations. This event was driven by an anomalously strong southward extension of the East Australian Current and its occurrence was at least 6.8 times more likely due to anthropogenic climate change. It has also been noted that a complete die-back of giant kelp (*Macrocystis pyrifera*) occurred in the coastal waters off eastern Tasmania during a warm weather event in 1988 (Sanderson, 1990) and an extreme ocean temperature event in 2000/2001 caused extensive die-back of kelp beds formed by the crayweed *Phyllospora comosa* off eastern Tasmania (Valentine and Johnson, 2004). More recent events caused mass deaths of Tasmanian Abalone in March 2010 (Craig Mundy, IMAS, pers. comm.) and deaths in Atlantic Salmon aquaculture populations in 2012 (Alistair Hobday, CSIRO, pers. comm.).

This study performs a systematic analysis of marine heatwaves off eastern Tasmania over the 23-year period from 1993 to 2015. A numerical ocean model is used to reconstruct the historical marine heatwave record in the region as well as high-resolution estimates of the associated water temperatures and circulation. We quantify the mean state and long term trends of marine heatwave properties, which are particularly strong off the southeast of Tasmania. The interannual variability of annual marine heatwave days is decomposed into two modes of variability and the East Australian Current is associated with nearly half of the observed variability. Finally we organise each of the detected marine heatwaves into one of 12 types, using an automated neural network approach. Each type has a unique combination of marine heatwave properties, spatial and seasonal distribution, and associated oceanic and atmospheric circulation patterns. This typology may be used to inform analysis of trends in different types of marine heatwaves, and to prepare management responses based on event types.

## 2. Data and methods

The data and methods are presented as follows: the high-resolution ocean model output for the continental shelf off eastern Tasmania (Section 2.1), the coarse-resolution estimates of the atmospheric and offshore ocean states (Section 2.2), the definition of marine heatwaves (MHWs) and their properties (Section 2.3), the calculation of annual MHW time series (Section 2.4), the Empirical Orthogonal Function analysis technique for the decomposition of the annual time series into modes of variability (Section 2.5) and the Self-Organising Maps analysis technique for the organisation of MHWs into a set of distinct types (Section 2.6).

### 2.1. ETAS ocean model

The historic ocean record off eastern Tasmania is derived from daily three-dimensional ocean temperatures and currents from the Eastern TASmania (ETAS) coastal ocean model which covers the 23-year period from 1993 to 2015 (Oliver et al., 2016). The ETAS model data provide an unprecedented high-resolution record of the marine climate variations off eastern Tasmania and represent our best estimate of the ocean state off eastern Tasmania. The ETAS model is based on the Sparse Hydrodynamic Ocean Code (SHOC; Herzfeld, 2006), a numerical ocean model well-suited to complex curvilinear grids with a large proportion of "land cells". The ETAS model covers the eastern continental shelf of Tasmania from South Cape in the south to just north of Eddystone Point in the northeast and seaward to just beyond the shelf break (~2500 m, Fig. 1a; Oliver et al., 2016). The model has a curvilinear grid, in a 200 × 120 grid cell configuration, with a horizontal resolution of ~1.9 km on average (Fig. 1b) and 43 $z$-levels in the vertical. Boundary forcing includes National Centers for Environmental Prediction (NCEP) Climate Forecast System (CFS) Reanalysis (CFSR, 1993–2010, Saha

et al., 2010) and CFS Version 2 analysis (CSFv2, 2011–2015, Saha et al., 2014) at the surface, and Bluelink ReANalysis (BRAN, version 3, 1/1/1993–31/7/2012, Oke et al., 2013) and OceanMAPS analysis (versions 2.0–2.2.1, 1/8/2012–31/12/2015; `wp.csiro.au/bluelink`) at the lateral boundaries. The model includes the influence of river runoff due to the two major rivers in the region; tidal forcing has not been included. The implications of excluding tidal variability include minor changes to seawater temperature variability (typically $\leqslant 0.5\,^{\circ}$C RMS difference; Oliver et al., 2016) and possibly altering the vertical structure of MHWs due to the absence of tidal mixing. The model provides daily, three-dimensional output for the 1993–2015 period and has been extensively validated against existing observations in the region (Oliver et al., 2016). Here, we have analysed surface and subsurface seawater temperatures and surface circulation.

The domain defined by the ETAS model has been divided into 12 regions in order to understand differences between regions impacted by MHWs (Fig. 1c). Boundaries between regions were defined by bathymetry, geography, and oceanography. Waters deeper than 200 m were termed "deep (D)", those between approximately 50 m and 200 m were termed "shelf (S)", and those in shallower water were given more descriptive names derived from local geography. Note that some of the inshore boundaries do not follow precisely the 50 m contour but were adjusted to close the regions in the bays and to reach the coast at the Freycinet, Tasman and South Cape Peninsulas and at Maria Island and Bruny Island. The "shelf" and "deep" zones were dominated by either the East Australian Current (EAC) in the north, the Zeehan Current (ZC) in the south, or their confluence (C) in between (Fig. 1d; see also Fig. 8 in Oliver et al. (2016) for seasonal surface circulation patterns). These zones were thus divided into six regions according to if they were EAC-dominated, ZC-dominated, or in the confluence and were either deep (D) or shelf (S), and named accordingly: EACD, EACS, CD, CS, ZCD, ZCS. The coastal zone is divided into six regions defined by their geography with appropriate names: north-east coast (NEC), Oyster Bay-Mercury Passage (OBMP), Frederick Henry and Norfolk Bays (FHNB), Storm Bay (SB), D'Entrecasteaux Channel (DC) and Huon Estuary (HE). The rivers and upper reaches of the Derwent and Huon estuaries were excluded from the 12 defined regions.

### 2.2. Large-scale oceanic and atmospheric states

Estimates of the ocean state outside the ETAS domain were provided by the Bluelink ocean forecasting system. Specifically, we examined daily fields of sea surface temperature (SST) and surface currents from the 1/10° BRAN and OceanMAPS products (Oke et al., 2013). The Bluelink reanalysis and analysis systems are data assimilative, including an array of both remotely-sensed and *in situ* ocean observations.

Estimates of the atmospheric state around Tasmania were provided by the NCEP CFS. Specifically, we examined daily-mean fields of 10 m air temperature and winds from CFSR and CFSv2 products (Saha et al., 2010, 2014). The CFSR (CFSv2) fields were defined on a grid with a horizontal resolution of 0.3° (0.2°). The CFS products are data assimilative, including an array of remotely-sensed and *in situ* atmosphere observations.

### 2.3. Marine heatwaves

Marine heatwaves (MHWs) have been identified from daily SST time series using the definition of Hobday et al. (2016a). A marine heatwave is defined as a "discrete prolonged anomalously warm water event at a particular location" with each of those terms (anomalously warm, prolonged, discrete) quantitatively defined and justified for the marine context. Specifically, "discrete" implies the marine heatwave is an identifiable event with clear start and end dates, "prolonged" means it has duration of at least five days, and "anomalously warm" means the water temperature is above a climatological threshold, defined here to be the seasonally-varying 90th percentile. Marine heatwaves were therefore identified as periods of time when temperatures were above the threshold for at least five consecutive days; two successive events with a break of two days or less between them were considered a single continuous event. The seasonally varying climatological mean and 90th percentile threshold were calculated for each day of the year using the pooled daily temperature values across all years within an 11-day window centred on the day, which were then smoothed using a 31-day moving window. The use of a seasonally-varying threshold allows for the detection of summer heatwaves as well as winter warm spells, both of which can have ecological impacts. This definition has been implemented as a freely available software tool in Python[1] and R.[2]

Sea surface temperatures from the ETAS model were spatially averaged over each of the regions defined in Section 2.1 to generate a set of 12 regional daily SST time series covering 1993–2015. Subsurface temperature at every model depth level over the same time period was also spatially averaged within each of the regions. The marine heatwave definition was then applied to each SST and subsurface temperature time series to detect all the marine heatwave events for each region, across all depths. The implication of spatially averaging SSTs and then performing the MHW calculation, as opposed to detecting MHWs directly from the pixel-based data, is to smooth away some of the high-frequency variability and thereby slightly increase average MHW duration at the expense of annual frequency. Nonetheless, this is a valid approach since we are interested in spatially-coherent MHW structures, rather than less coherent fine-scale features, as these are most likely to lead to significant ecological impacts.

Each marine heatwave event is assigned a set of properties, including duration, maximum and cumulative intensity, onset and decline rates and depth (Table 1; Hobday et al., 2016a). These metrics are defined as follows: "duration" is the time between the event's start and end dates, "maximum intensity" is the maximum temperature anomaly (measured relative to the climatological, seasonally-varying mean) over the duration of the event respectively, "cumulative intensity" is the integrated temperature anomaly over the duration of the event, and "onset rate" and "decline rate" are the rates of temperature increase and decline from the start date to the peak of the event and from the peak to the end date respectively. The "depth" of a marine heatwave is calculated by considering marine heatwave events at all subsurface model levels within the same region. The maximum depth over which a contiguous block of marine heatwave events occur simultaneously and connected with the surface event is defined as the "depth" of the event. Note that this maximum depth can occur at a time other than the time of maximum surface intensity.

### 2.4. Annual time series

Annual time series were calculated for each MHW property in each region. For duration, the intensity metrics, and depth this was the average of these properties across all events in each year; years with no events were marked as missing data. Two additional annual metrics were also calculated: "frequency", the count of events in each year, and "total MHW days", the sum of the durations of all events in each year. The annual mean and linear trend, estimated by Ordinary Least Squares including a 95% confidence interval, were calculated for each annual time series.

### 2.5. Empirical Orthogonal Function analysis

Empirical Orthogonal Function (EOF; e.g. Wilks, 2006) analysis is a statistical technique which accounts for the total variance of a set of variables by decomposing into linear combinations of those variables. Each linear combination, or EOF, corresponds to a statistically

[1] https://github.com/ecjoliver/marineHeatWaves.
[2] https://github.com/cran/RmarineHeatWaves.

**Table 1**
Marine heatwave (MHW) metrics, their units and descriptions, after Hobday et al. (2016a).

| Name | Units | Description |
|---|---|---|
| Duration | days | Time period between start and end of MHW |
| Maximum intensity | °C | Maximum temperature anomaly above climatology during the MHW |
| Cumulative intensity | °C days | Integral of temperature anomaly above climatology during the MHW, numerically equivalent to the sum of all daily intensity values |
| Onset rate | °C $day^{-1}$ | Rate of temperature change from the start to the peak of MHW |
| Decline rate | °C $day^{-1}$ | Rate of temperature change from the peak to the end of MHW |
| Depth | m | The maximum depth below the surface that a MHW penetrates |

uncorrelated mode of variability. For spatio-temporal data the EOF mode generally consists of a spatial pattern of weights and an associated principal component (PC) time series; the product of an EOF pattern and its PC time series is used to reconstruct the spatio-temporal variability associated with that mode alone. While EOF modes are statistical constructions, and therefore do not explicitly explain physical modes of variability, it is often the case that a small number of modes explain much of the variance and that important physical processes can be gleaned from these modes. Therefore, EOFs are often used as a "data reduction technique" where most of the variability is contained in these few modes.

We perform an EOF analysis on the 12 regional time series of total MHW days. This metric is chosen as it is the simplest representation of exposure to MHWs – e.g. more or longer events both lead to increases in MHW days. The linear trend is removed from each time series and then they are weighted by the area of that region before performing the EOF analysis. The regional oceanic and atmospheric circulation associated with each mode was obtained by projecting the higher resolution data (ETAS SST and surface circulation, Bluelink SST and surface circulation, NCEP air temperature and winds) onto the EOF modes, after the removal of the linear trend and seasonal cycle and conversion to annual mean time series.

### 2.6. Self-organising maps and a marine heatwave typology

Marine heatwaves were organised into a set of types using Self Organising Maps (SOMs; Kohonen, 1990, 1995). The SOM technique is a form of cluster analysis which uses an artificial neural network to produce a low-dimensional representation ("map") of high-dimensional input data. In that sense it is a form of dimension reduction and allows for a small number of patterns to be gleaned from a large data set. In oceanography and atmospheric science, SOMs have been used to distinguish flavours of El Niño–Southern Oscillation (Johnson, 2013), to organise coastal ocean circulation patterns off southeastern Tasmania (Williams et al., 2014), to explore heatwave patterns in Australia (Gibson et al., 2017) and categorise coastal MHWs off South Africa (Schlegel et al., 2017). Under a changing climate, different MHW types may become more or less frequent, as proposed for other climate modes.

The high-dimensional data set to be organised by the SOM consisted of the average oceanic and atmospheric anomaly states during each of the MHW events detected across all 12 regions (486 events in total). For each event the anomalous SST and surface circulation from ETAS and Bluelink as well as the anomalous air temperature and surface winds from NCEP were temporally averaged over the duration of that event. The domains used for the Bluelink and NCEP data were [144.85°E–149.85°E, 45.15°S–39.15°S] and [144.92°E–150.24°E, 45.12°S–38.87°S] respectively; the ETAS data were used over the whole model domain. Maps of the conditions for all events can be found in the Eastern Tasmania Marine Heatwave Atlas (Oliver et al., 2017b). Each variable (SST, zonal and meridional surface ocean currents, air temperature, zonal and meridional surface wind) was scaled by its standard deviation (across time and space) prior to the SOM analysis in order to weight each variable equally; after analysis the variables in the resultant map nodes were rescaled accordingly. A two-dimensional SOM was used in a $4 \times 3$ arrangement (12 nodes) and was initialised using the first two principal components of the data, ensuring reproducibility of the result (Agarwal and Skupin, 2008).

The choice of the number of nodes is important (Gibson et al., 2016). Too few nodes is insufficient to view the full range of possible states while too many leads to redundancy, with minimal differences between adjacent nodes. The choice of 12 nodes in a $4 \times 3$ arrangement led to only two nodes having patterns that were not statistically independent of each other ($p > 0.05$, two-sample $t$-test; Johnson, 2013). Arrangements with fewer nodes (e.g., $3 \times 3$, $3 \times 2$) had fewer independent patterns than the chosen $4 \times 3$ arrangement. However, the current arrangement ($4 \times 3$, 12 nodes) has two nodes that are not independent meaning we have effectively 11 independent patterns more than would be provided by the next-smallest arrangement ($3 \times 3$ arrangement, 9 nodes). Therefore, we erred on the side of providing a more comprehensive selection of patterns (maximum number of independent nodes) at the small expense of having two of the nodes be not independent.

The resultant SOM was analysed further to glean information about the distribution of MHWs across time and space, as well as associated circulation patterns. Each SOM node $(i,j)$ was associated with a set of MHWs $L_{ij}$. The oceanic and atmospheric circulation patterns as well as the MHW properties themselves were averaged across all events $L_{ij}$ for each node $(i,j)$. In addition, for each node $(i,j)$ we examined the proportion of events in $L_{ij}$ which ocurred in each climatological season and the distribution of these events across the 12 ETAS regions. The seasons were defined as summer (JFM), autumn (AMJ), winter (JAS) and spring (OND). Finally, these results were qualitatively summarised using oceanographic expertise in order to identify the unique MHW "type" associated with each SOM node.

## 3. Results

The results are presented as follows: the mean and linear trends of MHW properties (Section 3.1), their interannual variability (Section 3.2), and the organisation of MHWs into distinct types (Section 3.3).

### 3.1. Mean state and long-term trends

The mean state of MHW properties exhibits regional variations (Table 2). The frequency of events is between 1.5 and 2.0 annual events with generally higher frequencies in the southern nearshore regions (11 and 12). Mean MHW duration also varies considerably from ~7 days in the southern inshore to ~10–15 days in the shelf regions and ~14–18 days in the deeper offshore regions. MHW intensity generally increases towards the south with values <2 °C in the 3 northern-most regions and >2 °C further south. Cumulative intensity varies considerably across the region since it is influenced by both MHW intensity and duration, and it exhibits the spatial pattern of both; however, duration appears to play a dominant role and so the southern regions with shortest duration events also appear to have the smallest mean values of cumulative intensity. The total number of MHW days per year

**Table 2**
Mean state and linear trends in MHW properties for the 12 ETAS regions. Mean values are in units of annual event count (frequency), days (duration, total days), °C (maximum intensity), °C days (cumulative intensity), and m (depth). Trends are in the same units as the mean, per decade; bold values are statistically significant at the 5% level.

| Region | Frequency | Duration | Max. int. | Cum. int. | Total days | Depth |
|---|---|---|---|---|---|---|
| *Mean* | | | | | | |
| 1. EACS | 1.52 | 13.23 | 1.86 | 19.0 | 23.9 | 121 |
| 2. EACD | 1.87 | 17.73 | 1.84 | 27.7 | 26.7 | 152 |
| 3. CS | 1.65 | 14.75 | 2.30 | 26.0 | 25.4 | 90.8 |
| 4. CD | 1.87 | 16.30 | 2.09 | 28.0 | 28.5 | 162 |
| 5. ZCS | 1.61 | 10.71 | 2.03 | 15.4 | 25.4 | 93.1 |
| 6. ZCD | 1.74 | 13.84 | 2.13 | 23.7 | 30.3 | 185 |
| 7. NEC | 1.74 | 12.19 | 1.90 | 17.8 | 24.8 | 33.4 |
| 8. OBMP | 1.57 | 12.58 | 2.23 | 19.4 | 22.3 | 52.5 |
| 9. FHNB | 1.83 | 10.65 | 2.62 | 21.2 | 21.1 | 28.8 |
| 10. SB | 1.74 | 6.87 | 2.23 | 12.1 | 15.1 | 21.6 |
| 11. DC | 2.00 | 6.78 | 2.67 | 14.8 | 21.9 | 22.4 |
| 12. HE | 2.00 | 7.05 | 2.50 | 13.3 | 19.0 | 27.6 |
| *Trend (per decade)* | | | | | | |
| 1. EACS | **1.26** | −2.12 | −0.323 | −4.32 | 16.8 | 31.0 |
| 2. EACD | **1.72** | −5.75 | −0.0381 | −10.2 | **22.1** | 81.6 |
| 3. CS | **1.18** | −3.48 | −0.440 | −10.9 | 13.6 | **90.1** |
| 4. CD | **1.39** | −2.65 | −0.117 | −6.06 | **21.5** | 87.6 |
| 5. ZCS | **1.05** | **15.5** | −0.209 | **16.0** | **35.7** | **111** |
| 6. ZCD | **1.35** | 2.50 | −0.194 | 1.72 | 24.4 | 60.6 |
| 7. NEC | **1.68** | −2.00 | **−0.324** | −4.99 | **22.4** | 3.68 |
| 8. OBMP | **0.988** | 1.57 | **−0.519** | −0.818 | 13.2 | **22.4** |
| 9. FHNB | 0.435 | 3.47 | 0.00730 | 5.45 | 11.8 | **8.03** |
| 10. SB | **1.95** | 3.29 | 0.0488 | 4.62 | **21.2** | **25.6** |
| 11. DC | **2.77** | **5.11** | 0.0654 | **10.8** | **38.0** | **19.8** |
| 12. HE | **2.78** | 2.73 | −0.0500 | 4.62 | **30.5** | 17.5 |

is in the range of ~15–30 days with lowest values inshore to the south and largest values offshore in the deep regions. Average MHW depth is generally between 90 m and 185 m in the shelf and deep regions and between ~20–50 m in the nearshore regions, and this is strongly influenced by the maximum depth of the regions.

Long-term trends in marine heatwave properties were clearest in frequency, total MHW days, and depth (Table 2). MHW frequency exhibits a statistically significant ($p < 0.05$) positive trend across all regions, except region 9 (Frederick Henry-Norfolk Bay) and at a similar rate of change per decade as the mean MHW frequency. Total annual MHW days exhibits strong positive trends ($p < 0.05$) off southeastern Tasmania (regions 5 and 10–12) as well as along the northeast coast and in two of the offshore regions; as a relative fraction of the mean the trends are largest in magnitude in the southern nearshore regions (10–12). Significant ($p < 0.05$) positive trends in MHW depth were found for all regions south of the EAC-ZC confluence (inclusive), except for region 12. As with frequency, the magnitude of these trends (per decade) is comparable to that for the mean depth, indicating a corresponding deepening of MHWs off southeastern Tasmania. Duration, maximum intensity, and cumulative intensity only exhibit significant trends at two of the 12 regions and with little spatial coherence. We note that with a time series of this length, attribution of this trend to climate change is tenuous, however, these trends are against a background of sustained warming that has a clear climate change signal.

### 3.2. Interannual variability

Time series of the total annual MHW days demonstrate a large amount of interannual variability, including regional variation (Fig. 2). A number of the northern and offshore regions share peaks in MHW properties during 2001, 2003, 2007, 2010 an 2014 (regions 1–8). Independently, a number of the southeastern inshore and shelf regions share a period of heightened MHW days from 2012–2014 and a relatively quiescent period from 2002–2009 (regions 5 and 9–12).

An EOF analysis was performed to decompose the interannual variability into a set of EOFs, or modes. The first two modes together explain 79% of the total variance, with the first (second) mode explaining 49% (30%; Fig. 3), and they explain the two patterns noted in the previous paragraph. The first mode consists of large year-to-year variability in the total annual MHW days, with anomalies from the climatological average on the order of −20 to +40 days (Fig. 3a) distributed across the entire domain, although with less weight on the inshore and shelf regions off southeastern Tasmania (Fig. 3b). A projection of the regional atmospheric and oceanic circulation onto this mode indicates it is associated with southward along-shore circulation over the shelf and offshore, an anticyclonic eddy offshore to the southeast, warm ocean and air temperatures, and easterly winds (Fig. 4a and b).

The second mode consists of lower frequency variations in annual MHW days (Fig. 3c). Multi-year periods of persistent increased or decreased MHW days, up to ±40 days, were found with periods of increased MHW days during 1993–2000 and 2012–2014 and periods of decreased MHW days during 2003–2011 and 2015. This mode is expressed as a dipole pattern with a negative pole centred across the three northern regions and a positive pole centred across the southern and southeastern regions indicating that these broad regions exhibit the variability associated with this mode with opposite polarity (Fig. 3d). A projection of the regional atmospheric and oceanic circulation onto this mode indicates it is associated with relatively weak currents over the shelf, a train of cyclonic and anticyclonic eddies offshore, a dipole pattern of SSTs over the shelf, and northwesterly winds with warm air temperature over coastal areas of eastern and southeastern Tasmania (Fig. 4c and d).

### 3.3. A marine heatwave typology

The anomalous ocean and atmospheric states during each of the 486 MHWs were organised into 12 types using Self Organising Maps. The mean SSTs and surface circulation across all events in each type are shown in Fig. 5; the corresponding mean air temperature and surface winds are shown in Fig. 6. Nodes are identified in two dimensions using the identifier $(i,j)$ where $i$ runs from 1–4 (left-to-right in the figures) and $j$ from 1–3 (top-to-bottom), for a total of 12 nodes (types).

The nodes that occur most frequently (⩾10% of all events, see Table 3), meaning MHWs are more likely to be assigned to these nodes, lie in the four corners of the SOM and these represent the most distinct ocean–atmosphere patterns. In the ocean, there was a general pattern of increasing influence of the East Australian Current (southward flow) for lower $j$-nodes, i.e. increasing from the lower panels (high $j$) to the upper panels (low $j$) in Fig. 5. In the atmosphere, there was a general pattern of increasing influence of warm air temperatures for higher $i$-nodes, i.e. increasing from the left-most (low $i$) to the right-most (high $i$) panels in Fig. 6. Since these two features vary independently along the two axes of the SOM the corner nodes represent combinations of these features: strong EAC and weak air temperature anomalies (1,1), strong EAC and warm air temperature anomalies (4,1), weak EAC and strong air temperature anomalies (4,3), weak EAC and weak air temperature anomalies (1,3). The remaining nodes represent intermediate transitionary types between these four major types.

The nodes of the Self Organising Map have also been examined to determine the regional and seasonal distribution of constituent MHWs (Fig. 7) as well as mean MHW properties (Table 3) and the linear trend in annual MHW days associated with each node (Fig. 8). Each

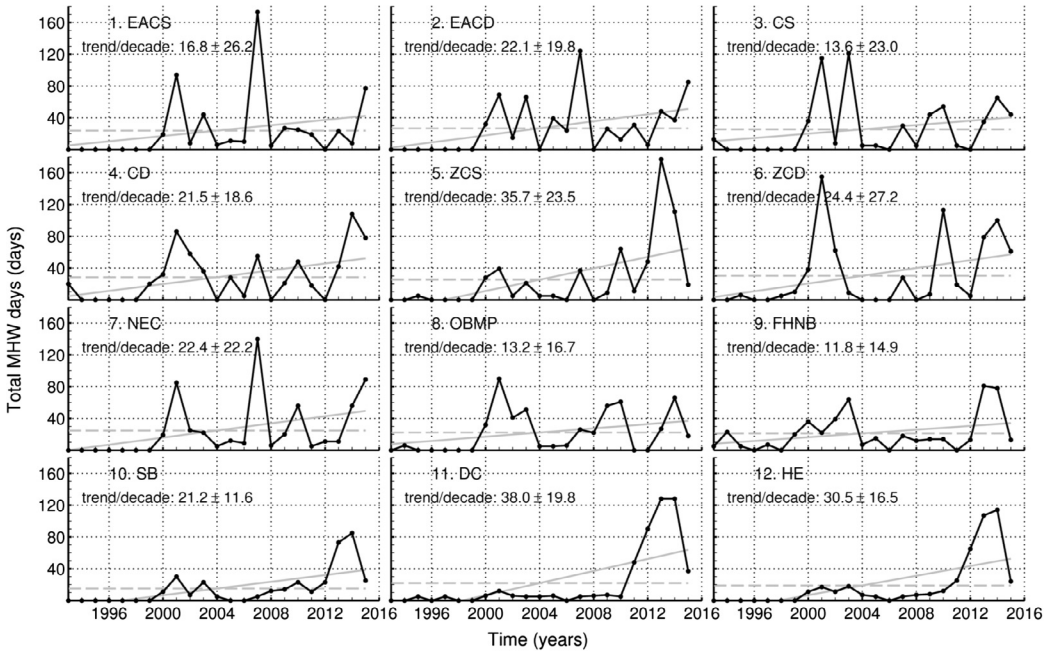


**Fig. 2.** Time series of total MHW days by region. Total annual MHW days are indicated by the black line, the mean by the dashed grey line, and the linear trend by the solid grey line (the trend is also printed in each panel, including a 95% confidence interval).

individual node is characterised in terms of ocean and atmospheric conditions, regional and seasonal distribution, and MHW properties (Appendix A). These descriptions have been qualitatively summarised in Table 4.

## 4. Discussion

We first summarise the results relating to the physical oceanogrphy, climate variability and change (Section 4.1) then discuss the ecological and management implications (Section 4.2).

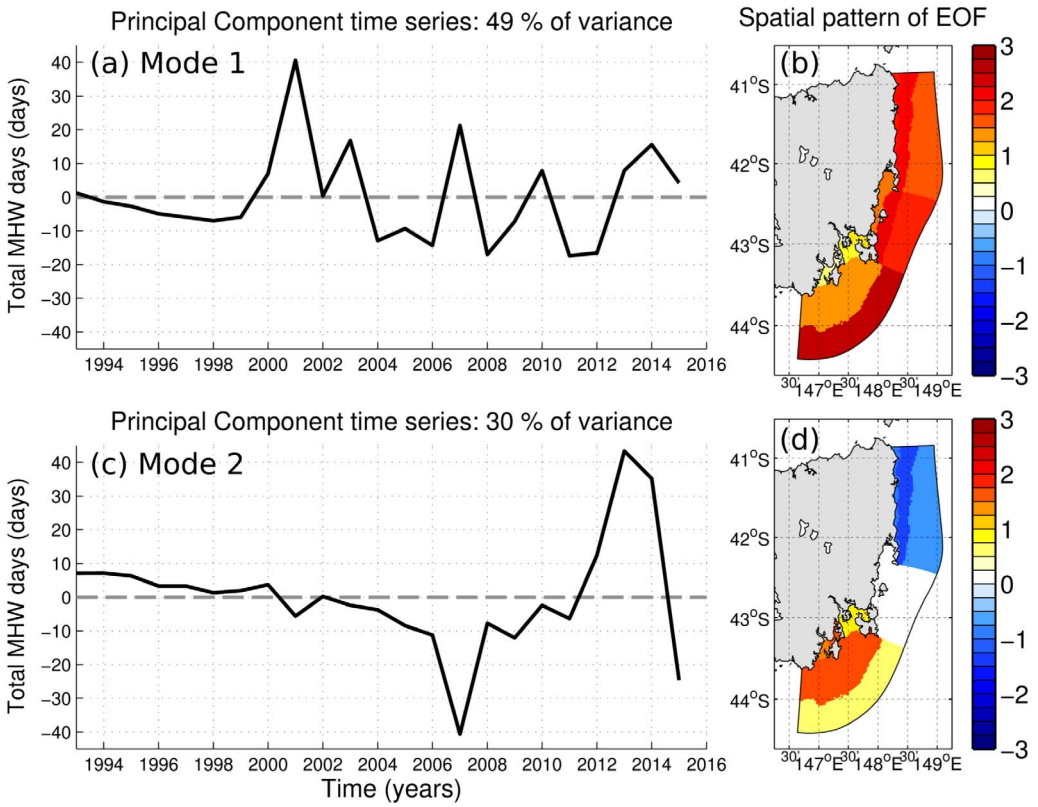


**Fig. 3.** First two EOFs (modes) of variability of total annual MHW days. The (a and c) principal component time series and (b and d) spatial patterns are presented for the first (a and b) and second (c and d) EOFs.

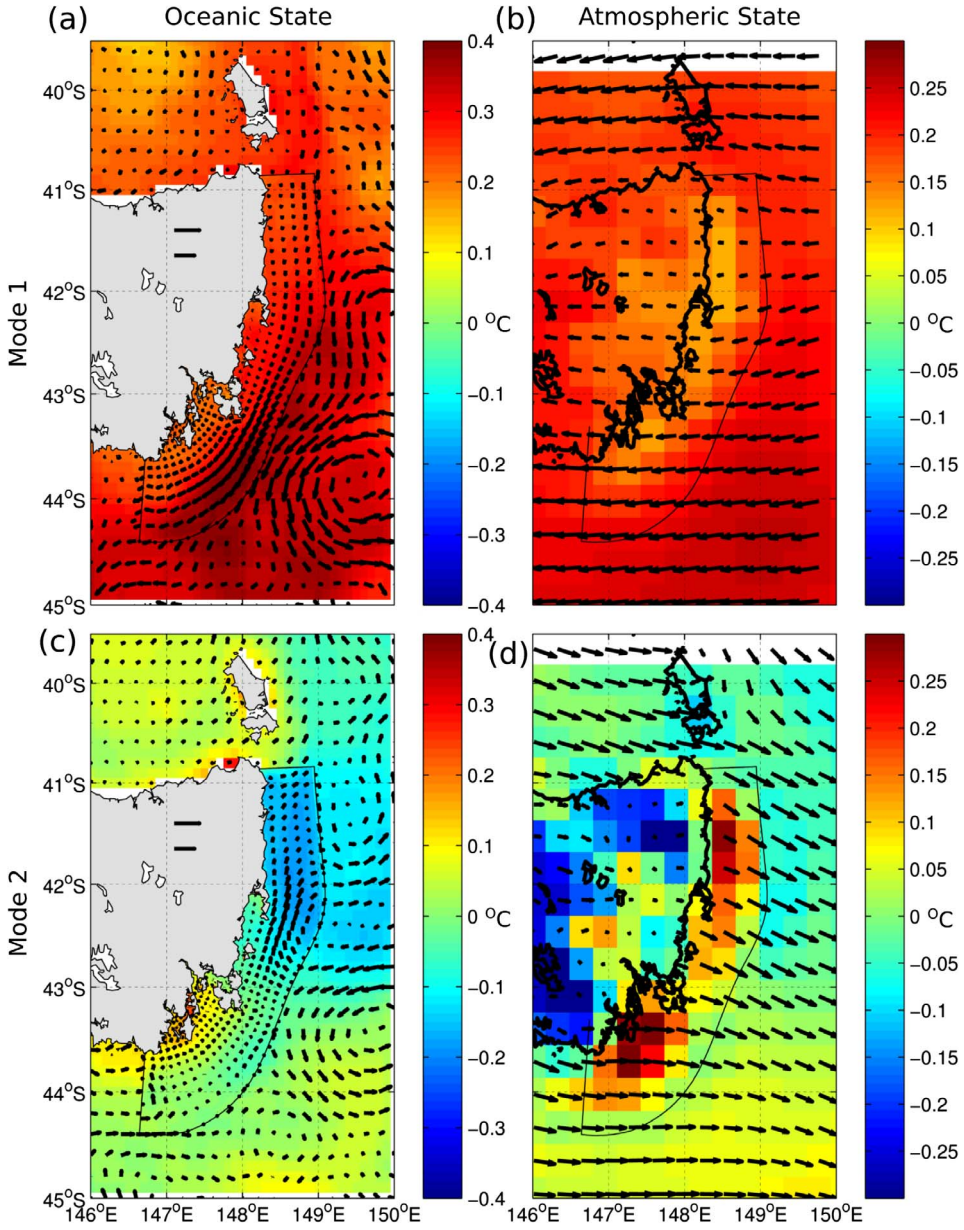


**Fig. 4.** Regional ocean and atmospheric circulation and temperature associated with the two modes of interannual variability. Presented are anomalies of sea surface temperature (colours, left), surface currents (arrows, left), air temperature (colours, right) and surface winds (arrows, right) after projection onto the (upper) first and (lower) second EOF modes of total annual MHW days. The two reference bars (over land) indicate (upper) an ocean current of 0.05 m $s^{-1}$ and (lower) a wind speed of 0.2 m $s^{-1}$. (For interpretation of the references to colour in this figure legend, the reader is referred to the web version of this article.)

### *4.1. Physical oceanography, climate variability and change*

We have presented the spatial and temporal distribution of marine heatwaves off eastern Tasmania including the mean state and linear trends, interannual variability, and an event typology. The mean state indicated a greater frequency and intensity of MHWs in the south of the domain, but with shorter durations; the opposite pattern is present over the remainder of the shelf. Linear trends indicated significantly increasing frequencies everywere – at a linear rate that doubles the mean state over a decade. In addition, significant increases in the annual count of MHW days as well as the penetration depth of MHWs were found for the nearshore regions off southeastern Tasmania. Strong interannual variability in the annual MHW days was evident and could be primarily decomposed into two modes of variability – the first associated with year-to-year variations in the East Australian Current and explaining nearly half of the variability, and the second associated with semi-persistent ~5-year variations in a dipole pattern over the shelf. Finally, the hundreds of MHW events spread across the 12 regions of the shelf were categorised into 12 types, each with its own set of MHW properties, regionality, seasonality and associated circulation patterns. Many types were associated with some combination of the East Australian Current, offshore anticyclonic eddies, warm air temperatures, and/or wind anomalies from northwesterly-to-easterly directions (inclusive clockwise). Notably, event-types were characteristically devoid of cool SSTs over the shelf, northward ocean currents, or wind anomalies from westerly or southerly directions.

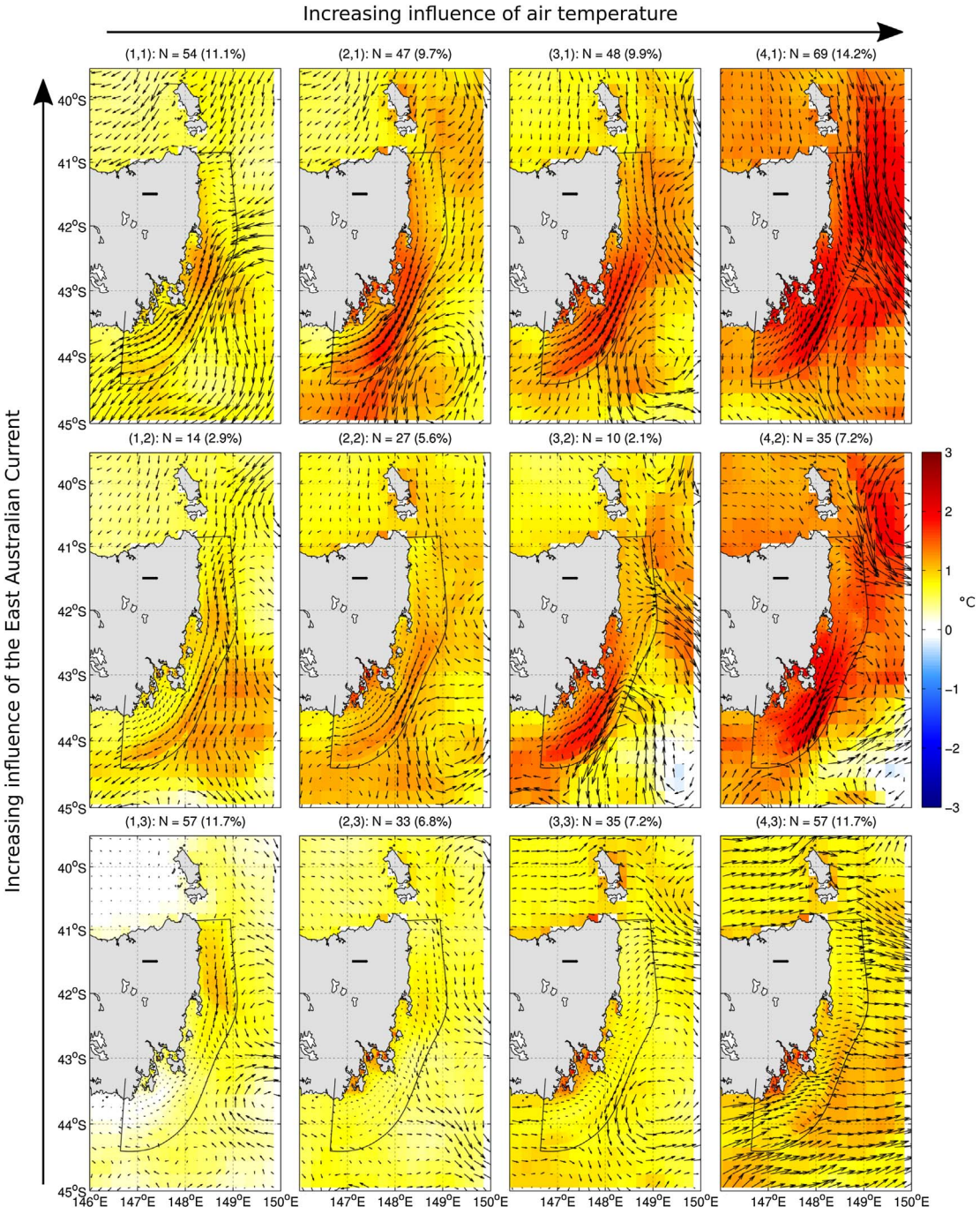


**Fig. 5.** Average ocean states during each of the 12 Self Organising Map (SOM) nodes. Colours (arrows) indicate SSTs (surface current) anomalies averaged across all events assigned to that node. The count of MHW events assigned to each node (and the proportion out of the total count) is indicated in the panel titles. The reference bar (over land) indicates an ocean current of 0.15 m $s^{-1}$. (For interpretation of the references to colour in this figure legend, the reader is referred to the web version of this article.)

These results have implications for understanding climate change in the region and the predictability of extreme ocean temperatures. That the southeastern part of Tasmania is a region of strong positive trends in marine heatwave properties is consistent with our understanding of this region as a front line of climate change. The east coast of Tasmania is the climatological boundary between the East Australian Current (EAC) and the Zeehan Current (ZC; Oliver et al., 2016), with the EAC being substantially warmer than the ZC and penetrating further south due to anthropogenic climate change (Ridgway, 2007; Oliver and Holbrook, 2014). Therefore, as the boundary between the two currents pushes south, regions formerly unexposed to the warm waters of the EAC will present a strong and significant response expressed through mean warming and increases in extremes – with likely ecological impacts. Associated with this long term warming are predictable interannual

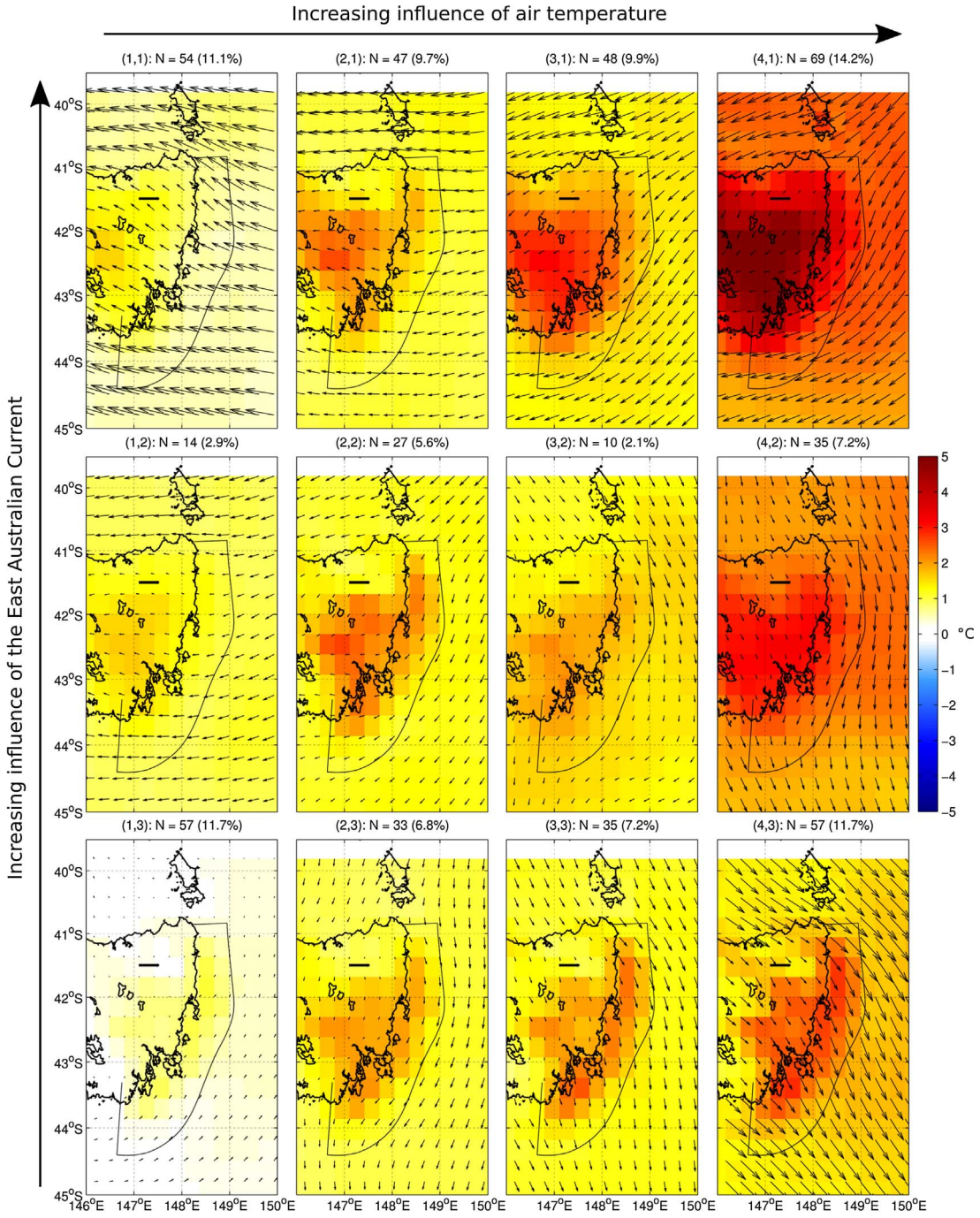


**Fig. 6.** Average atmospheric states during each of the 12 Self Organising Map (SOM) nodes. Colours (arrows) indicate surface air temperatures (surface wind) anomalies averaged across all events assigned to that node. The count of MHW events assigned to each node (and the proportion out of the total count) is indicated in the panel titles. The reference bar (over land) indicates a wind speed of 3 m $s^{-1}$. (For interpretation of the references to colour in this figure legend, the reader is referred to the web version of this article.)

variations in MHWs. As our analysis shows, large-scale year-to-year pulses of the potentially predictable EAC lead to interannual variations in the count of annual MHWs and these are superimposed on persistent multi-year variations. Finally, the set of 12 MHW types offer a form of "synoptic typing" in that they are associated with large-scale oceanic and atmospheric circulation patterns. If these patterns are present (or forecast) then the region may be predisposed to the occurrence of MHWs of the types described here. For example, if strong EAC conditions and northeasterly wind anomalies are forecast (using existing coarse-resolution forecast systems) during the Spring or Summer we might expect an increased likelihood of short and intense MHW events across the whole region (i.e. node (4, 1) – see Table 4), without having to explicitly forecast the coastal ocean itself at high-resolution. In contrast, the absence of these patterns indicates a predisposition for a lack of such MHWs in the region.

**Table 3**
Average MHW properties for each SOM node. The Frequency columns shows the total number of MHW events in each node, and in brackets the percentage from the total of 486 events. The remaining columns show the MHW durations (days), maximum intensities (°C), cumulative (°C days) and depths (m) averaged across all events in each node.

| Node | Frequency | Duration | Max. int. | Cum. int. | Depth |
|---|---|---|---|---|---|
| (1,1) | 54 (11.1%) | 18.4 | 1.84 | 26.2 | 113 |
| (2,1) | 47 (9.7%) | 14.7 | 2.25 | 24.0 | 127 |
| (3,1) | 48 (9.9%) | 10.5 | 2.29 | 19.8 | 85.4 |
| (4,1) | 69 (14.2%) | 7.5 | 2.46 | 15.3 | 98.9 |
| (1,2) | 14 (2.9%) | 25.0 | 2.07 | 36.2 | 102 |
| (2,2) | 27 (5.6%) | 17.1 | 2.21 | 29.4 | 86.3 |
| (3,2) | 10 (2.1%) | 14.8 | 2.27 | 26.4 | 112 |
| (4,2) | 35 (7.2%) | 10.5 | 2.39 | 20.7 | 111 |
| (1,3) | 57 (11.7%) | 14.9 | 1.63 | 19.9 | 128 |
| (2,3) | 33 (6.8%) | 18.2 | 1.80 | 22.9 | 114 |
| (3,3) | 35 (7.2%) | 16.3 | 1.92 | 23.3 | 60.4 |
| (4,3) | 57 (11.7%) | 8.5 | 1.94 | 13.5 | 82.0 |

### 4.2. Ecological and management implications

Ecological impacts associated with these MHWs can be revealed by short and long-term scientific studies, industry records, and citizen science observations. This historical MHW analysis for eastern Tasmania aims to shed light on previous ecological impacts for a range of researchers and marine users.

Rapid changes and tipping points may occur as a result of extreme events (Plagányi et al., 2014). In other regions, single MHWs have resulted in fish kills (e.g. Wernberg et al., 2013) and dramatic habitat changes (e.g. Wernberg et al., 2016; Hughes et al., 2017) that will likely persist for some time. Although there have been some climate-related long-term ecological changes in this study region (see Section 1), dramatic MHW impacts in this natural environment have been limited, although acute stress on aquaculture species does occur (Hobday et al., 2016b; Oliver et al., 2017a). The southerly location of Tasmania relative to the Australasian continent means that coastal species found here are likely to be living in the cooler end of the thermal preference spectrum (e.g. Stuart-Smith et al., 2015), and so even summer MHW changes in temperature have not exceeded critical temperature thresholds for the majority of local species (Oliver et al., 2017a). Conversely, milder winters due to climate-related warming, interspersed with MHWs, facilitate southward range expansion of species to Tasmania (e.g. sea urchin, *Centrostephanus rodgersii*, Ling et al., 2008; Ling et al., 2009b; numerous fish, Last et al., 2010; Robinson et al., 2015). For example, the establishment and gradual build-up of *Centrostephanus rodgersii* within Tasmanian kelp beds can lead to an ecological tipping-point (Ling et al., 2009a, 2015), which is reinforced by direct loss of kelps due to dieback during extreme conditions (e.g. Valentine and Johnson, 2003; Johnson et al., 2011; S. Ling, pers. obs.). In the present study, significant positive trends were found for MHW types (2,3) and (3,3) – winter MHWs which could be of importance for sea urchin larval development for larvae spawned in Tasmanian waters – and for type (4,1) – spring/summer MHWs associated with an EAC influence and conditions whereby greatest influx of *Centrostephanus* larvae from mainland Australia may occur.

There is also the potential for MHWs to impact the occurrence of viruses and harmful algal blooms, of great importance to the fisheries and aquaculture industries in Tasmania. For example, the 2015/16 MHW in the Tasman Sea led to an outbreak of Pacific Oyster Mortality Syndrome, a virus linked to warmer waters (Green et al., 2014), with significant impact on the oyster industry (Oliver et al., 2017a). On the other hand, the response of harmful algal blooms appears to be strongly dependent on water column stratification (Hallegraeff, 2010), which can be influenced by MHWs. The response of harmful algal blooms is further dependent on the seasonal timing of MHWs: i.e. along eastern Tasmania, warming at the end of the cool season (October-November) driving water temperatures above 15 °C could terminate blooms earlier, while conversely an earlier event (May-June) could enhance the growth season (Gustaaf Hallegraef, IMAS, pers. comm.). For example, a recent marine heatwave (Spring/Summer of 2017) in the Tasman Sea and south of Tasmania briefly touched the east coast of Tasmania, where it ended a paralytic shellfish poisoning bloom, allowing for the opening of the lobster fishery (Alistair Hobday, CSIRO, pers. comm.).

A workshop describing these Tasmanian MHW results was held in March 2017 with managers and marine resource users representing wild fisheries (lobster, abalone, finfish), and coastal aquaculture businesses (salmon, mussel, oyster). These and subsequent discussions revealed that managers still see MHW events largely as “natural” although the perception of being climate-related is increasing due to the general warming trend off eastern Tasmania (Holbrook and Bindoff, 1997; Ridgway, 2007), and commentary around eastern Tasmania MHW events in 2012 (Hodgkinson et al., 2014) and 2015 (Oliver et al., 2017a) where impacts on farmed species were reported. An increased scientific ability to do attribution studies also provides new climate-related evidence to marine stakeholders (e.g. Oliver et al., 2017a).

Importantly in this region, long term ocean warming trends and associated impacts are understood by recreational fishers (van Putten et al., 2014), commercial fishers (Nursey-Bray et al., 2012; Pecl et al., 2014) and aquaculture businesses (Spillman and Hobday, 2014), due to the pervasive nature of the long-term changes in distribution, abundance, and phenology already observed (Johnson et al., 2011; Frusher et al., 2014). The connection with the poleward-flowing East Australian Current for both long-term warming (Ridgway, 2007) and extremes (Oliver et al., 2014, 2017a; this paper) means that environmental understanding that stakeholders have based on long-term trends can be extended to include extremes such as MHWs, such as was recognised for the 2011 Western Australia marine heatwave (Metcalf et al., 2015). This positions regional fishery and aquaculture managers to use these historical data to understand past impacts as well as prepare for future risks. For example, aquaculture managers, with their greater system control, can implement a range of responses during MHW events, and the typological classification may help refine these choices (Spillman and Hobday, 2014). Cooler areas can be identified for different MHW types and some activities relocated to these areas, stocking densities can be reduced, and harvesting can be initiated earlier. Fishery and environmental managers with whom we discussed this work had a particular interest in the subsequent effects of MHW events such as delayed mortality, reduced recruitment or breeding success. These marine managers indicated that although they have few responses that they can apply during a MHW, they may make adjustments in subsequent years, for example, to harvesting levels, if effects persist at longer time scales. While the overwhelming focus of climate change related temperature effects is mortality of sensitive taxa, sub-lethal physiological stress leading to reproductive failure may have far greater consequences for population dynamics through recruitment failure. The typology of MHWs, when combined with retrospective analysis of ecological impacts might allow estimation of the subsequent ecological impacts for different MHW types, and thus inform management responses. Uncertainty about the relative effect of MHW duration and intensity on coastal ecological systems, and thus on the resources that stakeholders farm or harvest, necessitates additional study in partnership with these industries.

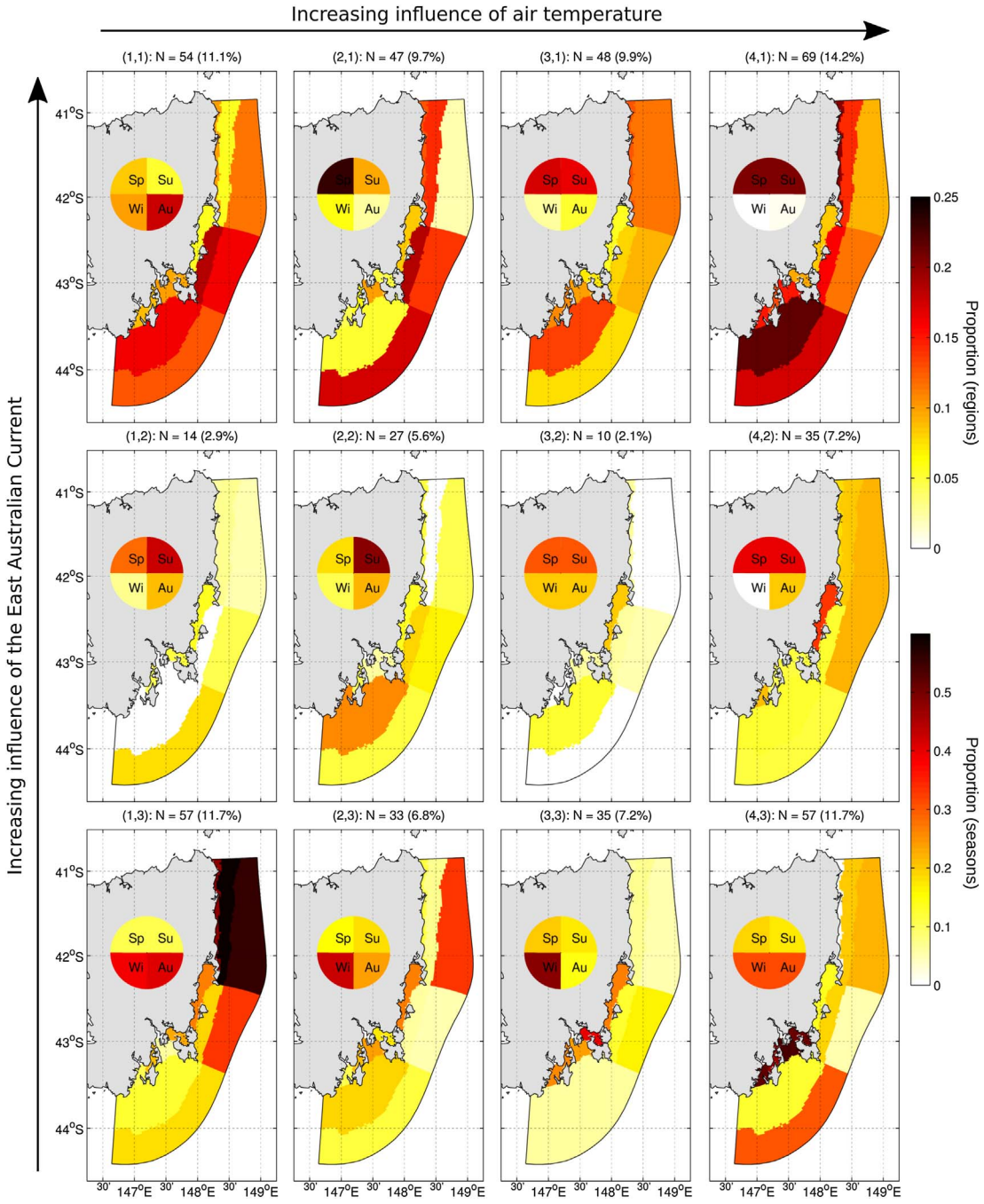


**Fig. 7.** Spatial and seasonal distribution of MHWs for each SOM node. The colour in each of the 12 regions indicates the proportion of events belonging to that node that occurs in each region (associated with upper right colourbar). The colour in each of the four quarter-circles indicate the proportion of events belonging to that node that occurs in each season (Su = Summer, Sp = Spring, Wi = Winter, Au = Autumn; associated with lower right colourbar). The count of MHW events assigned to each node (and the proportion out of the total count) is indicated in the panel titles. (For interpretation of the references to colour in this figure legend, the reader is referred to the web version of this article.)

In the meantime, we are working with managers and stakeholders to improve their ability to use these analyses, in areas such as risk-based management, harvest strategies, dynamic ocean management, coastal zoning and site selection. While stakeholders understand the need to develop mechanistic understanding supported by the retrospective analyses presented here, a range of discussions have revealed great interest in forecasts of MHW events. Forecasts of mean ocean state at a monthly temporal resolution are already delivered to ocean users in this region (Spillman and Hobday, 2014; Hobday et al., 2016b), which may contribute to demand for MHW predictions. Such predictions, which generally requires daily temporal resolution may be possible with new seasonal ocean forecast models (e.g. BOM ACCESS S, 25 km resolution), and distinguishing the type of MHW may provide additional prediction skill and inform the response options to users along this rapidly warming coastline.

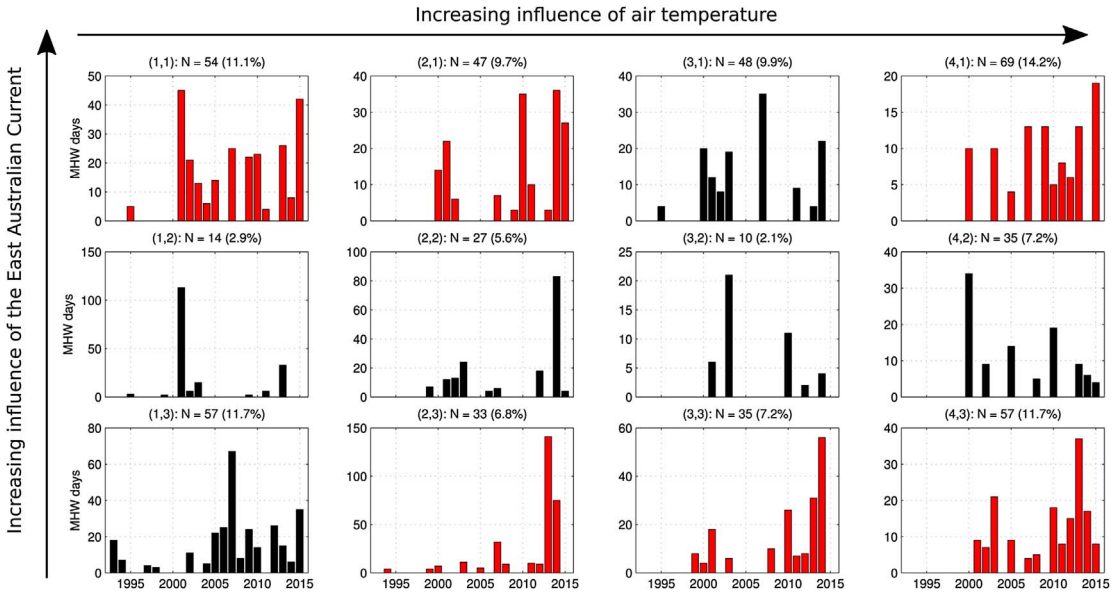


**Fig. 8.** Annual time series of MHW days associated with each SOM node. Panels with red bars indicate a statistically significant ($p < 0.05$) linear trend. The count of MHW events assigned to each node (and the proportion out of the total count) is indicated in the panel titles.

**Table 4**
Qualitative summary of the MHW typology. The regions commonly represented, seasonal occurrence, MHW properties, and associated ocean and atmospheric conditions are presented for each SOM node. The following definitions were used for the descriptive terms: frequent meant ⩾10%, infrequent meant ⩽5%, long (short) events lasted at least (most) 18 (10) days, intense (weak) events had a maximum intensity of at least (most) 2.2 °C (1.8 °C), deep events extended vertically over at least 110 m, the only node marked shallow had the shallowest events of all nodes. Acronyms are defined as: SE = Southeast, N = North, E = East, NE = Northeast, NW = Northwest, EAC = East Australian Current, AC = Anticyclonic. Region names are defined in Fig. 1.

| Node | Region | Season | MHW properties | Conditions |
|---|---|---|---|---|
| (1,1) | All | Autumn | Frequent, long, deep | Broad southward flow on and off the shelf, E-erly winds |
| (2,1) | All exc. SE coastal and NE offshore | Spring | Intense, deep | EAC flow over shelf, AC eddy off the SE, E-erly winds |
| (3,1) | All | Spring, Summer | Intense, fast onset and decline | EAC flow over shelf, AC eddy off the SE, NE-erly winds |
| (4,1) | All | Spring, Summer | Frequent, intense, short, fast onset | Strong EAC, large spatial scale, warm air, N-erly winds |
| (1,2) | ZCD, CD | Summer | Infrequent, long | EAC flow over shelf |
| (2,2) | ZCS, HE | Summer | Intense, fast decline | Broad southward flow over shelf, eddy off the SE |
| (3,2) | OBMP | All | Infrequent, intense, deep | Eddy train offshore |
| (4,2) | OBMP, northern, eastern offshore | Spring, Summer | Intense, deep | Eddy train offshore, warm air, N-erly winds |
| (1,3) | Northeast | Autumn, Winter | Frequent, weak, deep, slow onset and decline | Weak flow over shelf, eddy train offshore, weak atmosphere |
| (2,3) | EACD, OBMP, FHNB, DC | Winter | Weak, long, deep | Weak flow over shelf |
| (3,3) | Southeast coastal and OBMP | Winter | Shallow | Eddy off the SE, moderate strength Zeehan Current |
| (4,3) | Southeast coastal and ZCD | Autumn, Winter | Frequent, short, shallow | Strong Zeehan Current, warm air, NW-erly winds |

## Acknowledgements

This work was funded by a University of Tasmania (UTAS) Research Enhancement Granting Scheme (REGS) 2016 grant (Oliver, Holbrook, Ling, Mundy and Hobday, 2016, *Identifying historical marine heatwaves off eastern Tasmania*, UTAS REGS 2016, Grant No. O0023890). ECJO acknowledges funding from the Australian Research Council Centre of Excellence for Climate System Science (Grant No. CE110001028). NJH acknowledges funding from the Australian Research Council Centre of Excellence for Climate Extremes (Grant No. CE170100023). This paper makes a contribution to NESP Earth Systems Science and Climate Change Hub Project 2.3 (component 2) on the predictability of ocean temperature extremes. The ecological and management implications were partly informed by the "Marine Heatwaves Stakeholder Workshop: Marine heatwaves off eastern Tasmania: trends, variability, and typologies" held at the University of Tasmania on 20 March 2017, bringing together representatives from science (oceanographers, ecologists), industry (fisheries, aquculture), and Tasmanian state government departments. The ETAS ocean model data is available through the IMAS data portal (data.imas.utas.edu.au). The Bluelink ocean data products were provided by CSIRO; Bluelink is a collaboration involving the Commonwealth Bureau of Meteorology, the Commonwealth Scientific and Industrial Research Organisation and the Royal Australian Navy. The National Centers for Environmental Prediction (NCEP) Climate Forecast System (CFS) Reanalysis and Version 2 analysis data were provided by the Research Data Archive at the National Center for Atmospheric Research, Computational and Information Systems Laboratory.

## Appendix A. Description of the MHW types

Below are descriptions of each of the 12 MHW types (SOM nodes).

### A.1. Node (1, 1)

Node (1, 1) exhibits broad southward flow both on and off the shelf,

a hotspot of warm SSTAs (~1 °C) centred on the shelf between the Freycinet and Tasman Peninsulas, strong easterly winds and relatively low air temperature anomalies (⩽1 °C). This node occurs frequently (11.1% of all events) and MHWs are distributed across all regions, although perhaps more in the south than north. Events occurred predominantly in the Autumn and on average were long (18.4 days) and deep (113 m). Annual marine heatwave days associated with this node had a statistically significant linear increase of 8.95 days decade$^{-1}$.

### A.2. Node (2, 1)

Node (2, 1) exhibits broad southward flow both on and off the shelf (with offshore flow indicating an influence of the EAC), an anticyclonic eddy off southeastern Tasmania, warm SSTAs (up to ~2 °C) over the most of the shelf (but stronger in the south), moderate easterly wind anomalies and moderate air temperature anomalies 1–2.5 °C). This node occurs relatively frequently (9.9% of all events) and MHWs are distributed across most regions, excluding EACD and the nearshore regions of the southeast. Events occurred predominantly in the Spring and on average were intense (2.25 °C) and deep (127 m). Annual marine heatwave days associated with this node had a statistically significant linear increase of 8.56 days decade$^{-1}$.

### A.3. Node (3, 1)

Node (3, 1) exhibits broad southward flow both on and off the shelf (with offshore flow indicating an influence of the EAC), an anticyclonic eddy off southeastern Tasmania, warm SSTAs (up to ~2 °C) over the central and offshore southern parts of the shelf, strong northeasterly wind anomalies and moderate air temperature anomalies over the shelf (1–2 °C). This node occurs relatively frequently (9.7% of all events) and MHWs are distributed across most regions, excluding EACD and the nearshore regions of the southeast. Events occurred predominantly in the Spring and Summer and on average were intense (2.29 °C) with fast onset and decline rates (onset and decline rates not shown, see Oliver et al. (2017b) details).

### A.4. Node (4, 1)

Node (4, 1) exhibits strong southward flow both on and off the shelf (with a strong signature of the EAC offshore), very warm SSTAs (up to ~3 °C) over the entire shelf, strong northeasterly wind anomalies and warm air temperature anomalies over the shelf (2–4 °C). This node occurs the most frequently of all nodes (14.2% of all events) and MHWs are distributed across all regions. Events occurred only in the Spring and Summer and on average were the most intense (2.46 °C) and shortest (7.5 days) of all nodes, with fast onset rates. Annual marine heatwave days associated with this node had a statistically significant linear increase of 5.12 days decade$^{-1}$.

### A.5. Node (1, 2)

Node (1, 2) exhibits broad southward flow both on and off the shelf, warm SSTAs (~1 °C) predominantly away from the coast off the south of the shelf, moderate easterly wind anomalies and relatively low air temperature anomalies (~1 °C). This node occurs infrequently (2.9% of all events) and MHWs are distributed primarily in the offshore southeast (CD, ZCD) regions. Events occurred predominantly in the Summer and on average were the longest of all nodes (25.0 days).

### A.6. Node (2, 2)

Node (2, 2) exhibits southward flow over the shelf, an anticyclonic eddy off southeastern Tasmania, warm SSTAs (~1 °C) over most of the shelf, moderate northeasterly wind anomalies and moderate air temperature anomalies (1–2.5 °C). In this node occurs 5.6% of all events and MHWs are distributed primarily in the ZCS and HE regions. Events occurred predominantly in the Summer and on average were intense (2.21 °C) with fast decline rates.

### A.7. Node (3, 2)

Node (3, 2) exhibits a train of eddies running parallel to (and just offshore) the shelf edge, warm SSTAs (up to ~2 °C) over most of the southern half of the shelf, moderate northerly wind anomalies and moderate air temperature anomalies (1–2 °C). This node occurs the most infrequently (2.1% of all events) and most MHWs were in the OBMP region. Events occurred across all seasons (with a slight preference for Spring and Summer) and on average were intense (2.27 °C) and deep (112 m).

### A.8. Node (4, 2)

Node (4, 2) exhibits a train of eddies running parallel to (and just offshore) the shelf edge, very warm SSTAs (up to 1–2.5 °C) over most of the shelf, stong northerly wind anomalies and warm air temperature anomalies (2–3 °C). In this node occurs 7.2% of all events and most MHWs were in the OBMP region, with some across the northern regions and offshore to the east. Events occurred predominantly in the Spring and Summer and on average were intense (2.39 °C) and deep (111 m)

### A.9. Node (1, 3)

Node (1, 3) exhibits weak flow over the shelf, a train of eddies running parallel to (and just offshore) the shelf edge, SSTAs of ⩽1 °C increasing to the north, very weak wind anomalies and very low air temperature anomalies (⩽1 °C). This node occurs frequently (11.7% of all events) and MHWs are distributed primarily in the northern regions. Events occurred predominantly in the Winter and Autumn and on average were the weakest (1.63 °C) but deepest (128 m) of all nodes, with slow onset and decline rates.

### A.10. Node (2, 3)

Node (2, 3) exhibits weak flow over the shelf, SSTAs of ⩽1 °C over the shelf except in the coastal southeastern regions where SSTAs were up to 2 °C, moderate northerly wind anomalies and moderate air temperature anomalies (1–2 °C). In this node occurs 6.8% of all events and MHWs are distributed across the shelf with little spatial structure (highest numbers in EACD, OBMP, FHNB and DC). Events occurred predominantly in the Winter and on average were weak (1.80 °C), long (18.2 days) and deep (114 m). Annual marine heatwave days associated with this node had a statistically significant linear increase of 21.7 days decade$^{-1}$.

### A.11. Node (3, 3)

Node (3, 3) exhibits weak flow over most of the shelf except for a moderate strength Zeehan Current flowing eastward over the southern portion, an anticyclonic eddy off southeastern Tasmania, SSTAs of ⩽1 °C over the shelf except in the coastal southeastern regions where SSTAs were up to 2 °C, moderate-to-strong northerly wind anomalies

and warm air temperature anomalies over the shelf (1–3 °C). In this node occurs 7.2% of all events and MHWs are distributed predominantly in the coastal regions of the southeast (SB, FHNB, DC, HE) and east (OBMP). Events occurred predominantly in the Winter and on average were the shallowest (60.4 m) of all nodes. Annual marine heatwave days associated with this node had a statistically significant linear increase of 10.2 days decade$^{-1}$.

### *A.12. Node (4, 3)*

Node (4, 3) exhibits eastward flow over most of the shelf particularly in the south where there is a strong Zeehan Current entering from the west, warm SSTAs (~1 °C) over most of the shelf except in the coastal southeastern regions where SSTAs were up to 2–3 °C, strong northwesterly wind anomalies and warm air temperature anomalies over the shelf (2–3.5 °C). This node occurs frequently (11.7% of all events) and MHWs are distributed predominantly in the coastal regions of the southeast (SB, FHNB, DC, HE) the offshore region of the south (ZCD). Events occurred predominantly in Winter and Autumn and on average were short (8.5 days) and relatively shallow (82.0 m). Annual marine heatwave days associated with this node had a statistically significant linear increase of 8.44 days decade$^{-1}$.

## References


Agarwal, P., Skupin, A., 2008. Self-Organising Maps: Applications in Geographic Information Science. John Wiley & Sons.

Frusher, S.D., Hobday, A.J., Jennings, S.M., Creighton, C., D'Silva, D., Haward, M., Holbrook, N.J., Nursey-Bray, M., Pecl, G.T., van Putten, E.I., 2014. The short history of research in a marine climate change hotspot: from anecdote to adaptation in southeast Australia. Rev. Fish Biol. Fish. 24 (2), 593–611.

Garrabou, J., Coma, R., Bensoussan, N., Bally, M., Chevaldonné, P., Cigliano, M., Diaz, D., Harmelin, J.-G., Gambi, M., Kersting, D., et al., 2009. Mass mortality in Northwestern Mediterranean rocky benthic communities: effects of the 2003 heat wave. Global Change Biol. 15 (5), 1090–1103.

Gibson, P.B., Perkins-Kirkpatrick, S.E., Renwick, J.A., 2016. Projected changes in synoptic weather patterns over New Zealand examined through self-organizing maps. Int. J. Climatol. 36 (12), 3934–3948.

Gibson, P.B., Perkins-Kirkpatrick, S.E., Uotila, P., Pepler, A.S., Alexander, L.V., 2017. On the use of self-organizing maps for studying climate extremes. J. Geophys. Res.: Atmosph. 122 (7), 3891–3903.

Green, T.J., Montagnani, C., Benkendorff, K., Robinson, N., Speck, P., 2014. Ontogeny and water temperature influences the antiviral response of the Pacific oyster, Crassostrea gigas. Fish Shellfish Immunol. 36 (1), 151–157.

Hallegraeff, G.M., 2010. Ocean cliamte change, phytoplankton community responses, and harmful algal blooms: A formidable predictive challenge. J. Phycol. 46 (2), 220–235. http://dx.doi.org/10.1111/j.1529-8817.2010.00815.x.

Herzfeld, M., 2006. An alternative coordinate system for solving finite difference ocean models. Ocean Model. 14 (3), 174–196.

Hobday, A.J., Alexander, L.V., Perkins, S.E., Smale, D.A., Straub, S.C., Oliver, E.C., Benthuysen, J.A., Burrows, M.T., Donat, M.G., Feng, M., et al., 2016a. A hierarchical approach to defining marine heatwaves. Prog. Oceanogr. 141, 227–238.

Hobday, A.J., Pecl, G.T., 2014. Identification of global marine hotspots: sentinels for change and vanguards for adaptation action. Rev. Fish Biol. Fish. 24 (2), 415–425.

Hobday, A.J., Spillman, C.M., Paige Eveson, J., Hartog, J.R., 2016b. Seasonal forecasting for decision support in marine fisheries and aquaculture. Fish. Oceanogr. 25 (S1), 45–56.

Hodgkinson, J.H., Hobday, A.J., Pinkard, E.A., 2014. Climate adaptation in australias resource-extraction industries: ready or not? Reg. Environ. Change 14 (4), 1663–1678.

Hoffman, A.A., Sgro, C.M., 2011. Climate change and evolutionary adaptation. Nature 470, 479–485.

Holbrook, N.J., Bindoff, N.L., 1997. Interannual and decadal temperature variability in the southwest Pacific Ocean between 1955 and 1988. J. Climate 10 (5), 1035–1049.

Hughes, T.P., Kerry, J.T., Álvarez-Noriega, M., Álvarez-Romero, J.G., Anderson, K.D., Baird, A.H., Babcock, R.C., Beger, M., Bellwood, D.R., Berkelmans, R., et al., 2017. Global warming and recurrent mass bleaching of corals. Nature 543 (7645), 373–377.

Johnson, C.R., Banks, S.C., Barrett, N.S., Cazassus, F., Dunstan, P.K., Edgar, G.J., Frusher, S.D., Gardner, C., Haddon, M., Helidoniotis, F., et al., 2011. Climate change cascades: shifts in oceanography, species' ranges and subtidal marine community dynamics in eastern Tasmania. J. Exp. Marine Biol. Ecol. 400 (1), 17–32.

Johnson, J.E., Holbrook, N.J., 2014. Adaptation of Australia's marine ecosystems to climate change: using science to inform conservation management. Int. J. Ecol. 2014, 1–12.

Johnson, N.C., 2013. How many ENSO flavors can we distinguish? J. Climate 26 (13), 4816–4827.

Kelly, M.W., Sanford, E., Grosberg, R.K., 2011. Limited potential for adaptation to climate change in a broadly distributed marine crustacean. Proc. Roy. Soc. Lond. B: Biol. Sci. 279 (1727), 349–356. <http://rspb.royalsocietypublishing.org/content/279/1727/349>.

Kohonen, T., 1990. The self-organizing map. Proc. IEEE 78 (9), 1464–1480.

Kohonen, T., 1995. Self-Organizing Maps, vol. 30 Springer.

Last, P.R., White, W.T., Gledhill, D.C., Hobday, A.J., Brown, R., Edgar, G.J., Pecl, G., 2010. Long-term shifts in abundance and distribution of a temperate fish fauna: a response to climate change and fishing practices. Glob. Ecol. Biogeogr. 20, 58–72.

Lenton, T.M., Held, H., Kriegler, E., Hall, J.W., Lucht, W., Rahmstorf, S., Schellnhuber, H.J., 2008. Tipping elements in the Earth's climate system. Proc. Natl. Acad. Sci. 105 (6), 1786–1793.

Ling, S., 2008. Range expansion of a habitat-modifying species leads to loss of taxonomic diversity: a new and impoverished reef state. Oecologia 156 (4), 883–894.

Ling, S.D., Johnson, C., Frusher, S., King, C., 2008. Reproductive potential of a marine ecosystem engineer at the edge of a newly expanded range. Global Change Biol. 14 (4), 907–915.

Ling, S.D., Johnson, C.R., Frusher, S.D., Ridgway, K.R., 2009a. Overfishing reduces resilience of kelp beds to climate-driven catastrophic phase shift. Proc. Natl. Acad. Sci. 106 (52), 22341–22345.

Ling, S.D., Johnson, C.R., Ridgway, K., Hobday, A.J., Haddon, M., 2009b. Climate-driven range extension of a sea urchin: Inferring future trends by analysis of recent population dynamics. Global Change Biol. 15 (3), 719–731.

Ling, S.D., Scheibling, R.E., Rassweiler, A., Johnson, C.R., Shears, N., Connell, S.D., Salomon, A.K., Norderhaug, K.M., Pérez-Matus, A., Hernández, J.C., et al., 2015. Global regime shift dynamics of catastrophic sea urchin overgrazing. Phil. Trans. R. Soc. B 370 (1659), 20130269.

Metcalf, S.J., van Putten, E.I., Frusher, S., Marshall, N.A., Tull, M., Caputi, N., Haward, M., Hobday, A.J., Holbrook, N.J., Jennings, S.M., et al., 2015. Measuring the vulnerability of marine social-ecological systems: a prerequisite for the identification of climate change adaptations. Ecol. Soc. 20 (2).

Mills, K.E., Pershing, A.J., Brown, C.J., Chen, Y., Chiang, F.-S., Holland, D.S., Lehuta, S., Nye, J.A., Sun, J.C., Thomas, A.C., et al., 2013. Fisheries management in a changing climate lessons from the 2012 ocean heat wave in the Northwest Atlantic. Oceanography 26 (2), 191–195.

Nursey-Bray, M., Pecl, G.T., Frusher, S., Gardner, C., Haward, M., Hobday, A.J., Jennings, S., Punt, A.E., Revill, H., van Putten, I., 2012. Communicating climate change: climate change risk perceptions and rock lobster fishers, Tasmania. Marine Policy 36 (3), 753–759.

Oke, P.R., Sakov, P., Cahill, M.L., Dunn, J.R., Fiedler, R., Griffin, D.A., Mansbridge, J.V., Ridgway, K.R., Schiller, A., 2013. Towards a dynamically balanced eddy-resolving ocean reanalysis: BRAN3. Ocean Model. 67, 52–70.

Oliver, E.C., Benthuysen, J.A., Bindoff, N.L., Hobday, A.J., Holbrook, N.J., Mundy, C.N., Perkins-Kirkpatrick, S.E., 2017a. The unprecedented 2015/16 Tasman Sea marine heatwave. Nat. Commun. 8, 16101.

Oliver, E.C., O'Kane, T.J., Holbrook, N.J., 2015. Projected changes to Tasman Sea eddies in a future climate. J. Geophys. Res. 120 (11), 7150–7165.

Oliver, E.C.J., Herzfeld, M., Holbrook, N.J., 2016. Modelling the shelf circulation off eastern Tasmania. Continent. Shelf Res. 130, 14–33.

Oliver, E.C.J., Holbrook, N.J., 2014. Extending our understanding of South Pacific gyre 'spin-up': modeling the East Australian Current in a future climate. J. Geophys. Res. 119, 2788–2805.

Oliver, E.C.J., Lago, V., Holbrook, N.J., Ling, S.D., Mundy, C.N., Hobday, A.J., 2017b. Eastern Tasmania Marine Heatwave Atlas. Tech. rep., Institute for Marine and Antarctic Studies, University of Tasmania. < http://metadata.imas.utas.edu.au/geonetwork/srv/eng/metadata.show?uuid=20188863-0af6-4032-98f8-def671cdaa58 > .

Oliver, E.C.J., Wotherspoon, S.J., Holbrook, N.J., 2014. Projected Tasman Sea extremes in sea surface temperature through the 21st Century. J. Climate 27 (5), 1980–1998.

Pecl, G.T., Ward, T.M., Doubleday, Z.A., Clarke, S., Day, J., Dixon, C., Frusher, S., Gibbs, P., Hobday, A.J., Hutchinson, N., et al., 2014. Rapid assessment of fisheries species sensitivity to climate change. Clim. Change 127 (3–4), 505–520.

Perry, A.L., Low, P.J., Ellis, J.R., Reynolds, J.D., 2005. Climate change and distribution shifts in marine fishes. science 308 (5730), 1912–1915.

Plagányi, É.E., Ellis, N., Blamey, L.K., Morello, E.B., Norman-Lopez, A., Robinson, W., Sporcic, M., Sweatman, H., 2014. Ecosystem modelling provides clues to understanding ecological tipping points. Marine Ecol. Prog. Ser. 512, 99–113.

Ridgway, K.R., 2007. Long-term trend and decadal variability of the southward penetration of the East Australian Current. Geophys. Res. Lett. 34 (13), L13613.

Robinson, L.M., Gledhill, D.C., Moltschaniwskyj, N.A., Hobday, A.J., Frusher, S.D., Barrett, N., Stuart-Smith, J.F., Pecl, G.T., 2015. Rapid assessment of short-term datasets in an ocean warming hotspot reveals high confidence in potential range extensions. Global Environ. Change 31, 28–37.

Saha, S., Moorthi, S., Pan, H.-L., Wu, X., Wang, J., Nadiga, S., Tripp, P., Kistler, R., Woollen, J., Behringer, D., et al., 2010. The NCEP climate forecast system reanalysis. Bull. Am. Meteorol. Soc. 91 (8), 1015–1057.

Saha, S., Moorthi, S., Wu, X., Wang, J., Nadiga, S., Tripp, P., Behringer, D., Hou, Y.-T., Chuang, H.-y., Iredell, M., et al., 2014. The NCEP climate forecast system version 2. J.

Climate 27 (6), 2185–2208.
Sanderson, J.C., 1990. M.Sc. Thesis: Subtidal Macroalgal Studies in East and South Eastern Tasmanian Coastal Waters. University of Tasmania, Hobart, Australia.
Schlegel, R.W., Oliver, E.C.J., Perkins-Kirkpatrick, S., Kruger, A., Smit, A.J., 2017. Predominant atmospheric and oceanic patterns during coastal marine heatwaves. Front. Marine Sci. 4, 323.
Serrao-Neumann, S., Davidson, J.L., Baldwin, C.L., Dedekorkut-Howes, A., Ellison, J.C., Holbrook, N.J., Howes, M., Jacobson, C., Morgan, E.A., 2016. Marine governance to avoid tipping points: can we adapt the adaptability envelope? Marine Policy 65, 56–67.
Sloyan, B.M., O'Kane, T.J., 2015. Drivers of decadal variability in the Tasman Sea. J. Geophys. Res. 120 (5), 3193–3210.
Spillman, C.M., Hobday, A.J., 2014. Dynamical seasonal ocean forecasts to aid salmon farm management in a climate hotspot. Climate Risk Manage. 1, 25–38.
Stuart-Smith, R.D., Edgar, G.J., Barrett, N.S., Kininmonth, S.J., Bates, A.E., 2015. Thermal biases and vulnerability to warming in the world's marine fauna. Nature 528 (7580), 88.
Valentine, J.P., Johnson, C.R., 2003. Establishment of the introduced kelp Undaria pinnatifida in Tasmania depends on disturbance to native algal assemblages. J. Exp. Marine Biol. Ecol. 295 (1), 63–90.
Valentine, J.P., Johnson, C.R., 2004. Establishment of the introduced kelp undaria pinnatifida following dieback of the native macroalga Phyllospora comosa in Tasmania, Australia. Marine Freshwater Res. 55 (3), 223–230.
van Putten, I., Metcalf, S., Frusher, S., Marshall, N., Tull, M., 2014. Fishing for the impacts of climate change in the marine sector: a case study. Int. J. Climate Change Strategies Manage. 6 (4), 421–441.
Visser, M.E., 2008. Keeping up with a warming world; assessing the rate of adaptation to climate change. Proc. Roy. Soc. Lond. B: Biol. Sci. 275 (1635), 649–659. <http://rspb.royalsocietypublishing.org/content/275/1635/649>.
Wernberg, T., Bennett, S., Babcock, R.C., de Bettignies, T., Cure, K., Depczynski, M., Dufois, F., Fromont, J., Fulton, C.J., Hovey, R.K., et al., 2016. Climate-driven regime shift of a temperate marine ecosystem. Science 353 (6295), 169–172.
Wernberg, T., Smale, D.A., Tuya, F., Thomsen, M.S., Langlois, T.J., De Bettignies, T., Bennett, S., Rousseaux, C.S., 2013. An extreme climatic event alters marine ecosystem structure in a global biodiversity hotspot. Nat. Climate Change 3 (1), 78–82.
Wilks, D.S., 2006. Statistical Methods in the Atmospheric Sciences. Academic Press.
Williams, R.N., de Souza, P.A., Jones, E.M., 2014. Analysing coastal ocean model outputs using competitive-learning pattern recognition techniques. Environ. Model. Software 57, 165–176.